IEEE Access
Multidisciplinary | Rapid Review | Open Access Journal

Received July 25, 2019, accepted August 20, 2019, date of publication August 26, 2019, date of current version September 9, 2019.

Digital Object Identifier 10.1109/ACCESS.2019.2937623

Reliability Varying Characteristics of PV-ESS-Based Standalone Microgrid

XIAOTONG SONG, YUXIN ZHAO, JINGHUA ZHOU, AND ZHIPENG WENG
School of Electrical and Control Engineering, North China University of Technology, Beijing 100144, China

Corresponding author: Xiaotong Song (songxt@ncut.edu.cn)

This work was supported in part by the NSFC under Grant 51777002.

ABSTRACT Reliability is of critical importance for the microgrid (MG) and deserved more attention. Aiming at photovoltaics (PV) and energy storage system (ESS) based MG, the microturbine (MT), PV, ESS and comprehensive load (CL) which is composed of hourly time-varying component, stochastic component, and controllable component, are chronologically modeled and combined with model of load shedding minimization and sequential Monte Carlo (SMC) simulation algorithm. Then, the reliability assessment framework is developed and employed in the comprehensive case studies. Firstly, varying characteristics of reliability indices, including loss of load probability (LOLP), average service availability index (ASAI), system average interruption duration index (SAIDI), system average interruption frequency index (SAIFI) and customer average interruption duration index (CAIDI), over PV penetration are investigated, and the surge effect of SAIFI (SE-SAIFI) is especially put forward and studied, followed by the principle of PV capacity decision considering SE-SAIFI. Secondly, the clear pictures of reliability profiles over ESS sizes are depicted and analyzed, following with a novel method to reasonably decide ESS sizes based on the definition of expected hourly redundant power (EHRP). At last, reliability indices of multiple scenarios with different percentages of controllable load are calculated and the benefits of load management are analyzed in the viewpoint of reliability of standalone MG. Results of the case studies also confirm the necessities of reliability assessment during the MG planning and size optimization, and the validity of the methodologies developed in this work.

INDEX TERMS Standalone microgrid, energy storage system, sequential Monte Carlo simulation, reliability varying characteristics.

I. INTRODUCTION

Microgrids (MGs), supplying an efficient way for clean energy absorption and more flexible and smart power service, have attracted more and more interests [1]–[3]. Nowadays, a growing percentage of energy at home and abroad is employed to power the communities, smart industrial parks, isolated islands and remote rural settlements, *et al.*, not via traditional distribution grids but different types of MGs [4]–[6].

The challenges of intermittent nature of distributed generators (DGs), such as photovoltaics (PVs), wind turbines, etc., and novel energy management techniques have been necessitating the reliability assessment, especially on the standalone MGs. Different from grid-connected MGs or MG clusters, which are attracting more study interests on economic efficiency and reduction of fossil fuel usage [7], [8], standalone MGs are subject to more probable interruptions of power supply [9]. Therefore, energy storage systems (ESSs) have been playing an important role in the power supply-demand balance, mitigation of fluctuation of renewable powers and also the power supply continuity, considering that there is no power support from main grid for standalone MG [10].

The studies on reliability assessment of main grids [11] can give strong but still not enough support for MG reliability assessment, because of the absolutely different operation strategy, varying natures of the DGs, loads and applications of ESSs. A large number of literatures considered the reliability of MG as a criteria or constraint to deal with the MG planning or sizes optimization of DGs and/or ESSs. Reference [12] proposed a framework to economically optimize the deployment of DGs with a prerequisite of stipulated reliability. Reference [13] took the islanded operation

The associate editor coordinating the review of this article and approving it for publication was Eklas Hossain.

reliability which is represented by power mismatch, as a criteria to examine the feasibility of scheduling decisions in grid-connected mode. Similarly, Reference [14] combined the expected curtailed energy (ECE) index with the optimization model as part of objective function. In [15], battery size study was implemented in order to meet the reliability guarantees of island-capable MG, and loss of load probability (LOLP) was adopted as an index to denote reliability efficiency of battery size. It can be concluded from the aforementioned literatures that the consideration of reliability of MGs, especially the standalone ones or those with island-capable requirement, are of great importance to the economy and efficiency of MGs. Unfortunately, the reliability should be not only modeled as a 'criteria' or 'deadline' to validate the decisions of planning, grid augmentation, or power dispatch, *et al*., but also studied more comprehensively to get the overall profile and varying characteristics.

Reliability varying characteristics over the main elements of MG are attracting increasing but still not sufficient attentions. Reference [16] performed sensitivity studies of adequacy indices of standalone MG for spinning reserve, sizes of PV and ESS based on Monte Carlo (MC) simulation. In line with this work, [17] focused on the role of outage management strategy in reliability performance and demonstrated that MGs could gain reliability benefit from proper outage management strategy. Case studies implemented by [18] and [19] established the significant effects of RERs and BSS on the reliability indices as well as the economic efficiencies. Taking both the active and reactive power balance into consideration, Reference [20] analyzed the reliability improvement quantitatively due to the interconnection of distributed reactive sources (DRSs) and distributed energy storage resources (DESRs). In addition, Load management [21], [22] and demand response [23], play an important role in minimizing load curtailment and hence have been included in the reliability evaluation framework of MG.

From literature surveys, firstly, we can see that present research mainly deal with the reliability indices as criteria or constraints in the procedure of planning or energy dispatch. However, the reliability itself is a key and independent index of the power service and deserved a systematic and comprehensive study. Secondly, in order to comprehensively work out and compare the impacts of key elements, DGs, ESSs, load management, etc., should be considered in a unified framework rather than analyzed separately. Last, not only the reliability indices of probability, but also those of frequency & duration should be included in the study, for only the probability indices cannot depict the full view of MG reliability, and furthermore, frequency & duration indices may show different trends from probability indices, which has been demonstrated in the following discussion.

To fill these gaps, within the context of standalone MG, the reliability assessment methodology and varying characteristics of reliability indices are studied, following with comprehensive discussions. The contributions of the paper are as follows:

(a) A framework of sequential Monte Carlo (SMC) simulation including the models of MG and reliability indices of both probability and also frequency & duration was developed;

(b) Comprehensive study on a test standalone MG system is implemented to provide insights on reliability performance over sizes of PV and ESS, and controllable load percent; and

(c) The varying natures of probability indices and frequency & duration indices are thoroughly analyzed to promote a more reasonable planning decision when customers' requirements for the availability and continuity of power supply are delicately concerned.

The remainder of the paper is organized as follows. Section II formulates the stochastic models of MG and its elements, and SMC simulation algorithm procedures. In Section III, reliability varying characteristics are worked out and discussed based on intensive case studies, followed by conclusions of the paper in Section IV.

II. STOCHASTIC MODELS OF MG AND SMC ALGORITHM PROCEDURES

Analytical method and MC simulation are the basic methodologies in the reliability assessment of power system. Analytical method is usually more efficient than MC simulation in small systems, but will be limited or even forbidden by a) the rapidly growing computational burden along with the expansion of system dimensions or the increase of concerned stochastic issues, b) the loss of accuracy from ignoring high order contingencies, and c) the incompatibility with chronological factors of MG [24]. MC simulations, including the non-sequential Monte Carlo (NSMC) simulation and SMC simulation are preferred for the convergence performance independent on the system dimensions and capability to deal with the system behavior such as power dispatch, energy management and load shedding, *et al*., [25], [26]. In NSMC simulation, however, it is difficult to provide the frequency & duration indices since the random states of system components rather than the chronological state sequences are considered. On the contrary, the SMC simulation is attractive for its capability of dealing with the chronological and time-varying issues, such as load fluctuations, performance cycles of the components, *et al*., more accurately and efficiently [27]. In this paper, the need to work out not only probability indices but also frequency & duration indices, and the requirements of conveniently dealing with the stochastic and time-varying natures in MG favor the application of SMC simulation. Accordingly, the PV, microturbine (MT), ESS, load and the load-shedding strategy, considering their stochastic natures and operation performance, are modeled to be suitable for SMC simulation in this section. The effect of transmission elements, such as transformers, busbars, feeder sections, etc., are assumed as ideal elements, i.e., ignoring their failure rates and capacity constraints. However, the proposed models

below could be simply extended to consider the aforementioned constraints.

A. ELEMENTS' CHRONOLOGICAL OPERATION MODEL

The operation states of MG elements can be worked out by (1) [28].

$$\begin{cases} T_{on,ij} = -\left(\dfrac{1}{\lambda_i}\right)\ln u_{ij} \\ T_{off,ij} = -\left(\dfrac{1}{\mu_i}\right)\ln \xi_{ij} \end{cases} \tag{1}$$

Subscript i denotes the number of simulated element, and j denotes the number of operational sequences. For element i, $T_{on,ij}$ and $T_{off,ij}$ are the sampling operation time and repair time of j-th operational sequence. λ_i and μ_i are the failure rate and repair rate, respectively. u_{ij} and ξ_{ij} are random numbers generated from the continuous uniform distributions on the interval (0,1).

In order to get the operation status of MG, all the hourly 'on-off' sequences should be worked out and combined previously. Then the information combining probabilistic data and frequency& duration data are inherently contained and extracted accordingly.

B. PV POWER OUTPUT MODEL

PV power, with natures of intermittency and probability, can notably affect the reliability of MG, especially when the PV penetration is high. During the day time, power output of PV with Beta-probability density function, is modeled as (2) [29], [30].

$$f(P_{PV}^{available}(h)) = \frac{\Gamma(\alpha+\beta)}{\Gamma(\alpha)\Gamma(\beta)}\left(\frac{P_{PV}^{available}(h)}{P_{PV}^{max}}\right)^{\alpha-1}\left(1-\frac{P_{PV}^{available}(h)}{P_{PV}^{max}}\right)^{\beta-1} \tag{2}$$

where P_{PV}^{max} and $P_{PV}^{available}(h)$ are the PV power under maximum solar irradiance and the value available in the simulation hour h during day time, respectively. $f(P_{PV}^{available}(h))$ is the distribution function of $P_{PV}^{available}(h)$, α and β are the shape parameters of Beta distribution, and Γ is a Gamma function.

C. ESS MODEL

ESS plays an important role in the mitigation of renewable power fluctuation and keeping the consistency of power supply especially in the standalone MG. Battery is applied as ESS in this paper, and modeled based on state of charge (SOC) as below [21]:

$$SOC(h) = (1-\delta)SOC(h-1) + \frac{P_{ESSc}(h)\Delta t\eta_c}{E_{ESS}^{max}}F_{ESSc}(h) - \frac{P_{ESSd}(h)\Delta t}{E_{ESS}^{max}\eta_d}F_{ESSd}(h) \tag{3}$$

where $SOC(h)$ is the SOC of ESS in simulation step h, and initialized as 0.5 in this work. $P_{ESSc}(h)$ and $P_{ESSd}(h)$ are charging and discharging power of ESS in simulation step h, respectively. E_{ESS}^{max} is energy capacity of ESS. δ is the self-discharging rate and assumed as 0.001. η_c and η_d, identically assumed as 0.9, are the charging and discharging efficiency of ESS, respectively. $F_{ESSc}(h)$ and $F_{ESSd}(h)$ are the charging and discharging state variables of ESS, and valued in the following equations:

$$F_{ESSc}(h) = \begin{cases} 1 & when\ ESS\ in\ charging\ state \\ 0 & when\ ESS\ in\ discharging\ state \end{cases} \tag{4}$$

and

$$F_{ESSd}(h) = 1 - F_{ESSc}(h) \tag{5}$$

Still in (3), Δt is the simulation step. As it is set as 1 hour in this paper, (3) can be rewritten as follow:

$$SOC(h) = (1-\delta)SOC(h-1) + \frac{P_{ESSc}(h)\eta_c}{E_{ESS}^{max}}F_{ESSc}(h) - \frac{P_{ESSd}(h)}{E_{ESS}^{max}\eta_d}F_{ESSd}(h) \tag{6}$$

D. COMPREHENSIVE LOAD MODEL

In this paper, the hourly time-varying load model combined with the stochastic nature and performance of load management, comprehensive load (CL), denoted as $P_{LOAD}(h)$ is developed and modeled as follow:

$$P_{LOAD}(h) = P_{L\_t}(h) + P_{L\_rand}(h) + P_{L\_cb}(h) \tag{7}$$

where $P_{L\_t}(h)$, $P_{L\_rand}(h)$ and $P_{L\_cb}(h)$ are hourly time-varying component [27], stochastic component [31], and controllable component [32], respectively. $P_{L\_t}(h)$ and $P_{L\_rand}(h)$ are specified as (8), (9).

$$P_{L\_t}(h) = P_{year,peak} \times P_{month}(m(h)) \times P_{hour}(h) \tag{8}$$

$$f(P_{L\_rand}) = \frac{1}{\sqrt{2\pi}\sigma_{LOAD}}\exp\left(-\frac{(P_{L\_rand}-\mu_{LOAD})^2}{2\sigma_{LOAD}^2}\right) \tag{9}$$

In (8), $P_{year,peak}$ is the annual peak load and P_{month} is the percentage of monthly load in terms of the annual peak. Similarly, $P_{hour}(h)$ is the percentage of hourly load in terms of monthly peak. $m(h)$ is the month related to the simulation hour h. As expressed in (9), load uncertainty component P_{rand} is modeled by normal distribution function, and its expectation value and standard deviation are μ_{LOAD} and σ_{LOAD}, respectively. Controllable loads $P_{cb}(h)$, represented by contracted bands of possible reduction of the scheduled demand, are predetermined by agreement between the MG operator and the customers [32]. When power insufficiency occurs in simulation step h, the load $P_{ctr}(h)$ within contracted bands will be curtailed.

E. MINIMIZATION OF LOAD SHEDDING MODEL

Different energy scheduling strategies will lead to different operating decisions and also different results of reliability assessment. When it comes to the standalone MGs,

obj.

$$Min\{P_{curtail}(h)\} \tag{10}$$

$$\text{s.t. } P_{MT}(h) + P_{PV}(h) + P_{ESSd}(h) = P_{L\_t}(h) + P_{L\_rand}(h) + P_{L\_cb}(h) - P_{ctr}(h) - P_{curtail}(h) + P_{ESSc}(h) \tag{11}$$

$$0 \le P_{MT}(h) \le P_{MTmax} F_{MT}(h) \tag{12}$$

$$0 \le |P_{MT}(h) - P_{MT}(h)| \le \Delta P_{MT} \tag{13}$$

$$0 \le P_{PV}(h) \le P_{PV}^{available}(h) F_{PV}(h) \tag{14}$$

$$0 \le P_{ESSd}(h) \le P_{ESSd}^{max} F_{ESS}(h) F_{ESSd}(h) \tag{15}$$

$$0 \le P_{ESSc}(h) \le P_{ESSc}^{max} F_{ESS}(h) F_{ESSc}(h) \tag{16}$$

$$SOC_{min} \le \left\{ (1-\delta) SOC(h-1) + \frac{P_{ESSc}(h)\eta_c}{E_{ESS}^{max}} F_{ESSc}(h) - \frac{P_{ESSd}(h)}{E_{ESS}^{max}\eta_d} F_{ESSd}(h) \right\} \le SOC_{max} \tag{17}$$

$$0 \le P_{curtail}(h) \le P_{L\_t}(h) + P_{L\_rand}(h) \tag{18}$$

$$0 \le P_{ctr}(h) \le P_{L\_cb}(h) \tag{19}$$

the main consideration usually is to achieve the supply-demand balance and avoid or minimize the load curtailment if unavoidable.

Different from the cost-efficient [17] or environment-friendly [33] energy scheduling strategies, for example, a load curtailment minimizing model is developed to reschedule the generation output of DGs, battery charging/discharging power, and at last the load curtailment when necessary. The reliability indices resulted from the load curtailment minimizing model is adopted in the study of the reliability varying characteristics over different factors, since the aforementioned strategy of load curtailment shows a more clear and straightforward direction to the inherency of reliability, and is formulated as below:

h in the expression (10)-(19), as shown at the top of this page, denotes the simulation hour. In (10), the objective function is to minimize the load curtailment, i.e., $P_{curtail}(h)$. (11)-(19) are the constraints expressions, where (11) is power balance constraint, (12) is MT capacity constraint, (13) is MT ramping up/down constraints, (14) is PV available power constraint, (15), (16) and (17) are ESS discharging power, charging power and SOC constraints, respectively, (18) is the load curtailment constraint and (19) is load control constraint.

$P_{MT}(h)$ and $P_{PV}(h)$ denote power output of MT and PV, $P_{ESSd}(h)$ and $P_{ESSc}(h)$ denotes the ESS discharging power and charging power, respectively. $F_{MT}(h)$, $F_{PV}(h)$, and $F_{ESS}(h)$ are the binary states variables resulted from SMC simulation, representing the normal states when equivalent to 1, and fault states when equivalent to 0. P_{MTmax} is the capacity of MT, with the maximum ramping up/down capacity of ΔP_{MT}. P_{ESSd}^{max} and P_{ESSc}^{max} are the maximum discharging and charging power of ESS, respectively, and $SOC_{\min}$ and $SOC_{\max}$ are the minimum and maximum permissible SOC value of ESS.

F. RELIABILITY INDICES AND CONVERGENCE CRITERIA

In order to depict the overview of MG reliability, LOLP and average service availability index (ASAI), categorized as indices of probability, as well as system average interruption duration index (SAIDI, in hour/customer. year), system average interruption frequency index (SAIFI, in interruptions/customer. year) and customer average interruption duration index (CAIDI, in hour/customer. interruption), categorized as indices of frequency & duration are both adopted. Comprehensive interpretations of these indices are given in [11], [20], [34] and [35]. It should be noted that, the reliability indices of system rather than those of customer load points are referred, for the reliability varying characteristics of MG system as a whole are focused and studied in this paper.

The coefficient of variation β is used to denote the convergence of SMC simulation, and calculated as below:

$$\beta = \frac{\sqrt{V(F_R)/H}}{E(F_R)} \tag{20}$$

where $V(F_R)$ and $E(F_R)$ are the variance and expected value of reliability test function F_R, respectively. H is the total number of simulation hour steps.

G. PROCEDURES OF RELIABILITY ASSESSMENT ALGORITHM

A reliability assessment algorithm based on SMC simulation has been developed. Comprehensively considering the impacts of MT, PV, ESS, CL, etc., reliability profile of MG can be depicted by implementing the algorithm. The algorithm procedures graphically are shown as flowchart in Fig. 1.

Based on the aforementioned algorithm, a reliability evaluation program for MG has been coded in MATLAB language on the platform of MATLAB-R2014b. With this program, a test system built in Section III is modeled and chronologically simulated, and its reliability varying characteristics are studied thereafter.

III. CASE STUDIES

A. TEST SYSTEM AND CALCULATING ASSUMPTIONS

A test system of PV-ESS based standalone MG, schematically shown in Fig. 2, is applied as the background of reliability assessment.

The following data and assumptions are applied in the case studies.

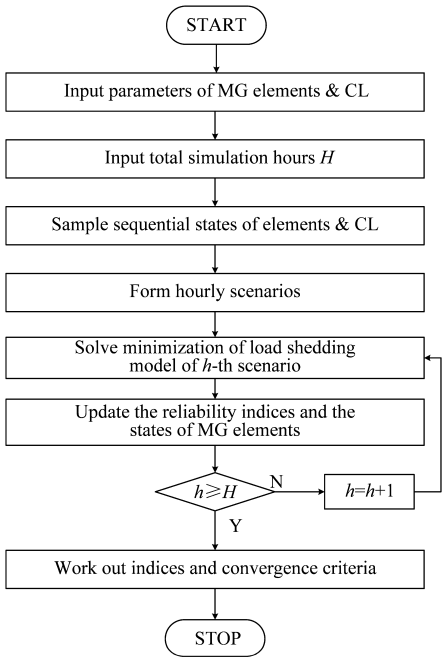

FIGURE 1. Flowchart of SMC simulation based algorithm for reliability assessment of MG.

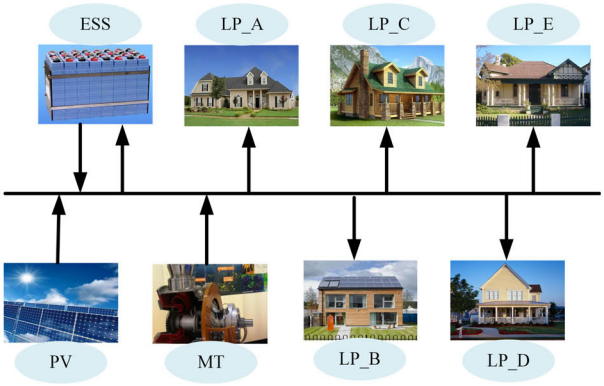

FIGURE 2. A schematic diagram of the PV-ESS based standalone MG for case studies.

(1) Annual Peak Load of the load points LP_A, LP_B, LP_C, LP_D and LP_E are identical with those of LP19, LP20, LP21, LP22 and LP23 of Feeder 4 in IEEE-RBTS BUS6 [36], and collected in Tab. 1. Percentages of monthly load in terms of the annual peak P_{month}, and the percentages of hourly load in terms of monthly peak $P_{hour}(h)$ are specified in Tab. 2 and Tab. 3 [37]. It should be noted that, hourly load variation parameters are given by time interval of 15 minutes in [37] and the parameters of first 15 minutes of every hour are selected in this paper as $P_{hour}(h)$ of different load points to model the behavioral patterns of energy consumers. Expectation value μ_{LOAD} and standard deviation σ_{LOAD} of load uncertainty component, referred in (9) are assumed as 0 and ten percent of hourly load, respectively. Then the profile of CL in a year is worked out and shown in Fig. 3.

(2) The failure rate, repair rate and repair duration of MT are assumed as 0.2 *occurrences per year*, 0.125 *occurrences per hour* and 8 *hours* respectively [37]. Failure rates of PV, and ESS are assumed as zero in the following case studies, i.e., $F_{PV}(h) = F_{ESS}(h) \equiv 1$, considering that the sizes of PV

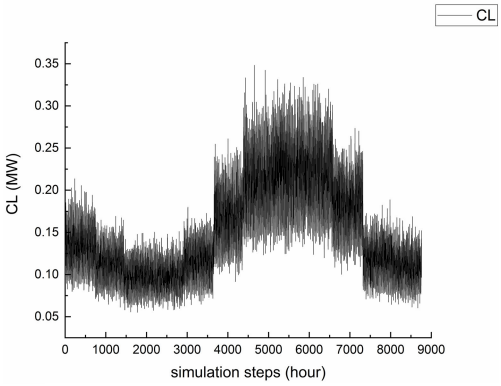

FIGURE 3. Curve of annual chronological CL with stochastic and hourly time-varying natures.

TABLE 1. Annual peak load data.

Load points	$P_{year,peak}$ (MW)
LP_A	0.2776
LP_B	0.5025
LP_C	0.7375
LP_D	0.2831
LP_E	0.7965

TABLE 2. Monthly load percentages in terms of annual peak.

Months	Percentages	Months	Percentages
1	0.5989	7	0.9422
2	0.4973	8	1
3	0.4356	9	0.9695
4	0.4343	10	0.8081
5	0.5126	11	0.5305
6	0.7530	12	0.4861

TABLE 3. Hourly load percentages in terms of monthly peak.

Time intervals	Percentages	Time intervals	Percentages
0:00-1:00	0.7407	12:00-13:00	0.9133
1:00-2:00	0.6923	13:00-14:00	0.9531
2:00-3:00	0.6527	14:00-15:00	0.9392
3:00-4:00	0.6212	15:00-16:00	0.9489
4:00-5:00	0.5845	16:00-17:00	0.9758
5:00-6:00	0.5972	17:00-18:00	0.9893
6:00-7:00	0.6079	18:00-19:00	1
7:00-8:00	0.6227	19:00-20:00	0.9921
8:00-9:00	0.6410	20:00-21:00	0.9554
9:00-10:00	0.6939	21:00-22:00	0.9104
10:00-11:00	0.7498	22:00-23:00	0.8467
11:00-12:00	0.8621	23:00-00:00	0.8154

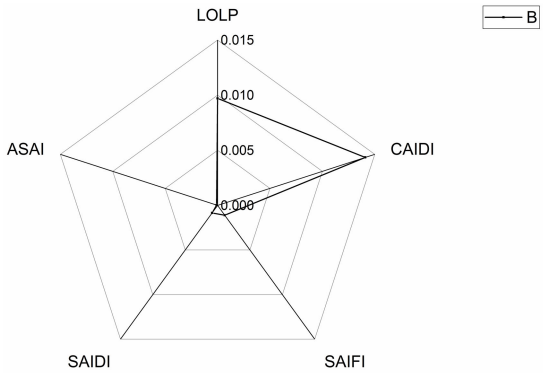

FIGURE 4. Coefficients of variation of different reliability indices within the convergence criteria (0.015) from SMC simulation of 10 years.

and ESS contribute much more to the reliability indices than their failure rates. However, the ignored failure rates could be simply included when necessary, by updating $F_{PV}(h)$ and $F_{ESS}(h)$ according to the hourly 'on-off' sequences of PV and ESS.

(3) Capacity of MT is assumed as 1.6 MW to provide the MG with consistent power supply and a fairly reasonable level of reliability, and sizes of PV and ESS are specified in the following study.

B. CONVERGENCE PERFORMANCE

Adequate computation cost is needed to get an acceptable coefficient of variation β. When $\beta < 0.015$, it is assumed that convergence criteria is reached in this paper. Here, PV capacity is assumed as 0.4 MW, and power capacity and energy capacity of ESS are assumed as 0.1 MW and 1.0 MWh, respectively. Then reliability assessment of the test system is implemented and the convergence performance is investigated accordingly. As shown in Fig. 4, the coefficients of variation of different indices are all less than 0.015 when the total simulation period reaches 10 years, i.e., 87600 hours. Consequently, the results presented below are computed from simulation of 87600 hours, then the results will be discussed with the same accuracy.

C. RELIABILITY PERFORMANCE OVER PV PENETRATION

As shown in Tab. 4, three scenarios, I, II and III, are defined by changing the sizes of ESS, i.e., energy capacity and charging & discharging power capacity (represented as 'Power capacity' for simplification in Tab. 4). Charging and discharging efficiency are both assumed as 0.9, and permissible SOC range is 0.2-0.9.

With the incremental steps of 0.2 MW, the capacity of PV varies from 0.4 MW to 6.2 MW. As shown in Fig. 5, the curves of reliability indices are worked out and numbered by I, II and III, according to the numbers of scenarios in Tab. 4.

Fig. 5 shows that, PV capacity imposes different impacts to different indices. From curves of LOLP-I, ASAI-I and SAIDI-I, it is observed that the probability and total duration time per year of load interruption will be decreased, while the

TABLE 4. ESS sizes of different scenarios.

Scenarios	Energy capacity (MWh)	Power capacity(MW)
I	1	0.1
II	3	0.5
III	3	1

TABLE 5. Reliability indices over different percentages of controllable load at LP_C.

Controllable Percentages	LOLP	CAIDI	SAIFI	SAIDI	SAIFI
0	0.0729	6.15	95.45	585.61	0.9133
10	0.0694	5.97	93.80	556.09	0.9365
20	0.0656	5.58	97.49	526.02	0.9400
30	0.0623	5.22	97.04	499.67	0.9430
40	0.0601	5.18	93.50	485.94	0.9445
50	0.0577	4.98	92.42	462.48	0.9472
60	0.0525	4.59	93.67	417.63	0.9523
70	0.0476	4.26	90.42	378.82	0.9568
80	0.0450	4.03	91.37	359.57	0.9590
90	0.0412	3.69	90.33	330.64	0.9623
100	0.0419	3.77	89.90	339.76	0.9612

decreasing rate reduces along with the increase of PV capacity, even gradually to zero approximately. From Fig. 5 (a)-(c), the range of PV capacity can be roughly subdivided into 3 subintervals, i.e., extremely insufficient (0.4-1.0), insufficient (1.0-2.0) and redundant interval (2.0-6.2) for scenario I. From the viewpoint of reliability efficiency, the reasonable capacity of PV can be determined accordingly.

Moreover, the reliability can be further improved, when necessary, by optimization of ESS sizes for example, rather than increasing the PV capacity. The reliability curves denoted by I, II and III, derived from different ESS sizes in Tab. 5, respectively, show that ESS with reasonable size can make full use of the PV capacity to obtain a higher reliability level.

It should be also noted that the curves of SAIFI-I and CAIDI-I show fluctuant profiles during the increase of PV capacity. In the extremely insufficient interval (0.4-1.0), the load disruption frequency, i.e., SAIFI increases along with the increase of PV capacity, but at the same time the mean disruption duration of each frequency, i.e., CAIDI decreases. The similar varying performance can also be found from curves of SAIFI-II and CAIDI-II in the interval (0.4-0.8) instead. It is referred as **'surge effect of SAIFI'** (SE-SAIFI) over PV capacity in this paper, which should be carefully taken into consideration in the decision of PV capacity.

In order to give further information and explanation of SE-SAIFI, the operation sequences from 5864 h to 5876 h, namely, 9:00 to 21:00 on 31th Aug. of the first simulation year, are explicitly shown in Fig. 6. Because of the redundancy of power supply from 9:00 to 12:00, ESS is charged continuously in this time interval. During 12:00 to 21:00, however, PV and MT can't cover the load anymore, due to the increase of load and decrease of PV output. Obviously,

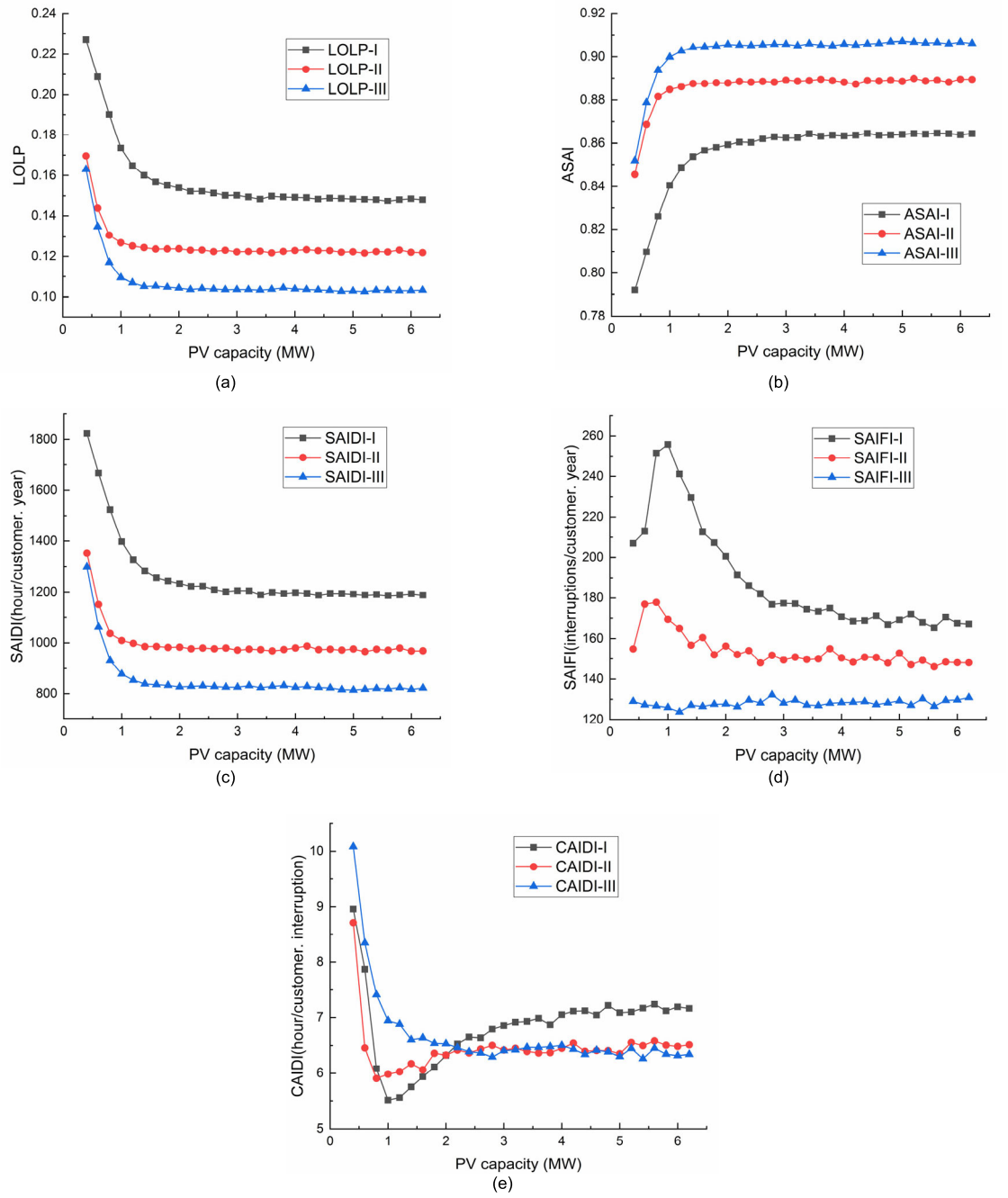

FIGURE 5. Reliability performance over varying PV capacities with consideration of different ESS sizes denoted as I, II and III: Along with increase of PV capacity, indices of (a) LOLP, (b) ASAI and (c) SAIDI improve steadily at a decreasing rate, and change evidently due to the variation of ESS sizes. (d) SE-SAIFI occurs when PV capacity is extremely insufficient and is depressed by upgrading ESS sizes. (e) CAIDI curve presents a valley correspondingly when SE-SAIFI occurs.

ESS is expected to discharge and compensate power gap. The test function of LOLP, denoted as $F_{LOLP}(h)$, turns to 1 (i.e., power deficiency) from 0 (i.e., power redundancy) at 13:00, then turns over again at 14:00, and rises back to 1 at 15:00.

It is seen that, the power interruption period from 13:00 to 21:00 is split into two intervals at the point of 14:00. This case can be helpful to understand SE-SAIFI. When the PV power is relatively small, as in interval (0.4-1.0) of SAIFI-I, or interval (0.4-0.8) of SAIFI-II, the increase of PV capacity will lead to more splits in the curve of $F_{LOLP}(h)$ as exemplified in Fig. 6, rather than reduce of load disruption occasions, resulting in a larger SAIFI and a smaller CAIDI accordingly. Nevertheless, when PV capacity exceeds the turning point of extremely insufficient interval, 1.0MW of curve SAIFI-I for example, the increased PV capacity is large

enough to partially eliminate the load disruption occasions with larger probabilities. Namely, SAIFI will be decreased accordingly.

It is obvious that the PV capacity should be greater than the turning point of extremely insufficient interval to avoid SE-SAIFI. By studying the curves of SAIFI-I, SAIFI-II and SAIFI-III, it is also worth mentioning that ESS with adequate size can depress the SE-SAIFI. The SE-SAIFI interval of curve SAIFI-II is smaller than that of curve SAIFI-I, and SE-SAIFI of SAIFI-III is almost vanished due to ESS with enough size. To draw a conclusion, the size of PV should be determined at least to overcome SE-SAIFI, with the consideration of ESS sizes.

D. RELIABILITY PERFORMANCE OVER ESS SIZES

Based on the developed program, reliability performance over different ESS sizes are studied. In this subsection, PV capacity is assumed as 2.6 MW and kept constant as a prerequisite for the following reliability calculations. According to the analysis in Subsection C, the PV capacity is large enough to present less influence on the variety of reliability indices. Hence, the reliability varying characteristics only resulting from changes of ESS sizes can be clearly investigated. With energy capacity varying from 1.0 MWh to 10.8 MWh with incremental steps of 0.2 MWh, and charging/discharging power capacity varying from 0.1 MW to 3 MW with incremental steps of 0.1 MW, the contour diagrams of reliability indices are worked out and shown in Fig. 7.

It can be seen from Fig. 7 that the reliability indices are improved continuously along with the increase of ESS energy capacity when the ESS power capacity is large enough. However, the improvement of reliability will be constrained to some extent by only increasing ESS energy capacity if the ESS power capacity is insufficient. Taking Fig. 7(a) as an example, with the constant ESS power capacity of 0.4 MW, the LOLP decreased marginally from 0.0902 to 0.0894, by increasing ESS energy capacity from 7 MWh at point P_1 to 10.4 MWh at point P_2. When the ESS power capacity is 1.5 MW and kept constant, however, the shift from point P_3 to point P_4, with identical ESS energy capacity to P_1 and P_2, respectively, will lead to an evident improvement of LOLP from 0.0535 to 0.0039. Similar varying characteristics can also be found when other diagrams in Fig. 7 are investigated. Then, a novel method is proposed by defining **expected hourly redundant power** (EHRP) in (21)-(23), as shown at the bottom of this page, to determine the reasonable size of ESS.

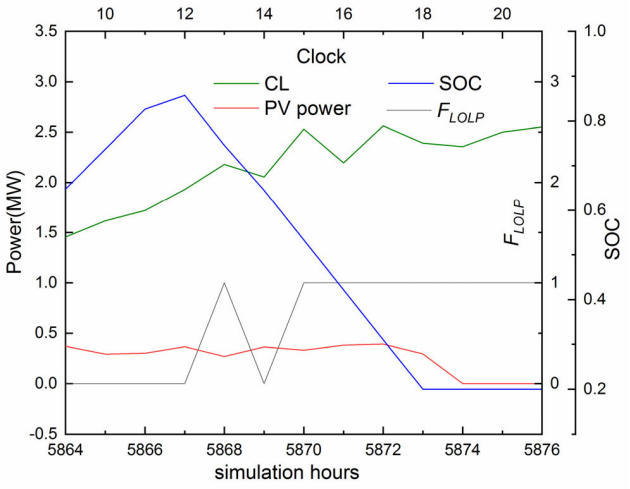

FIGURE 6. A case of split of F_{LOLP} curve during the operation sequences from 5864-hour to 5876-hour (i.e., 9:00 to 21:00 on 31th Aug. of the first simulation year) shown as an explanation of SE-SAIFI. Notice that due to the relatively small sizes of PV and ESS, the power interruption period from 13:00 to 21:00 is split into two intervals at the point of 14:00 when the fluctuation of CL occurs.

EHRP can be worked out by SMC simulation without heavy computational burden, because the load shedding strategy and ESS performance are not necessarily considered. Since the reliability requirements favor the capacity of ESS that is large enough to absorb the redundant power as much as possible, index of EHRP will give a reasonable reference for ESS power capacity decision. Based on the assumptions in subsection A of Section III, EHRP is determined as 1.352 MW. Then the capacity reference lines which are parallel with the energy capacity axis, with constant power capacity of EHRP, are drawn in Fig. 7.

It should be noted that, the contour lines are divided into two parts by capacity reference lines, i.e., upper part and lower part. Upper part of contour lines are approximately vertical to the energy capacity axis, and lower part of

$$\mathrm{EHRP} = \frac{1}{H'}\sum_{h=1}^{H} F_{EHRP}(h) \times \left(P_{MTmax}F_{MT}(h) + P_{PV}^{available}(h)F_{PV}(h) - P_{LOAD}(h)\right) \tag{21}$$

where,

$$F_{EHRP}(h) = \begin{cases} 0, & when P_{MTmax}F_{MT}(h) + P_{PV}^{available}(h)F_{PV}(h) \le P_{LOAD}(h) \\ 1, & when P_{MTmax}F_{MT}(h) + P_{PV}^{available}(h)F_{PV}(h) > P_{LOAD}(h) \end{cases} \tag{22}$$

and

$$H' = \sum_{h=1}^{H} F_{EHRP}(h) \tag{23}$$

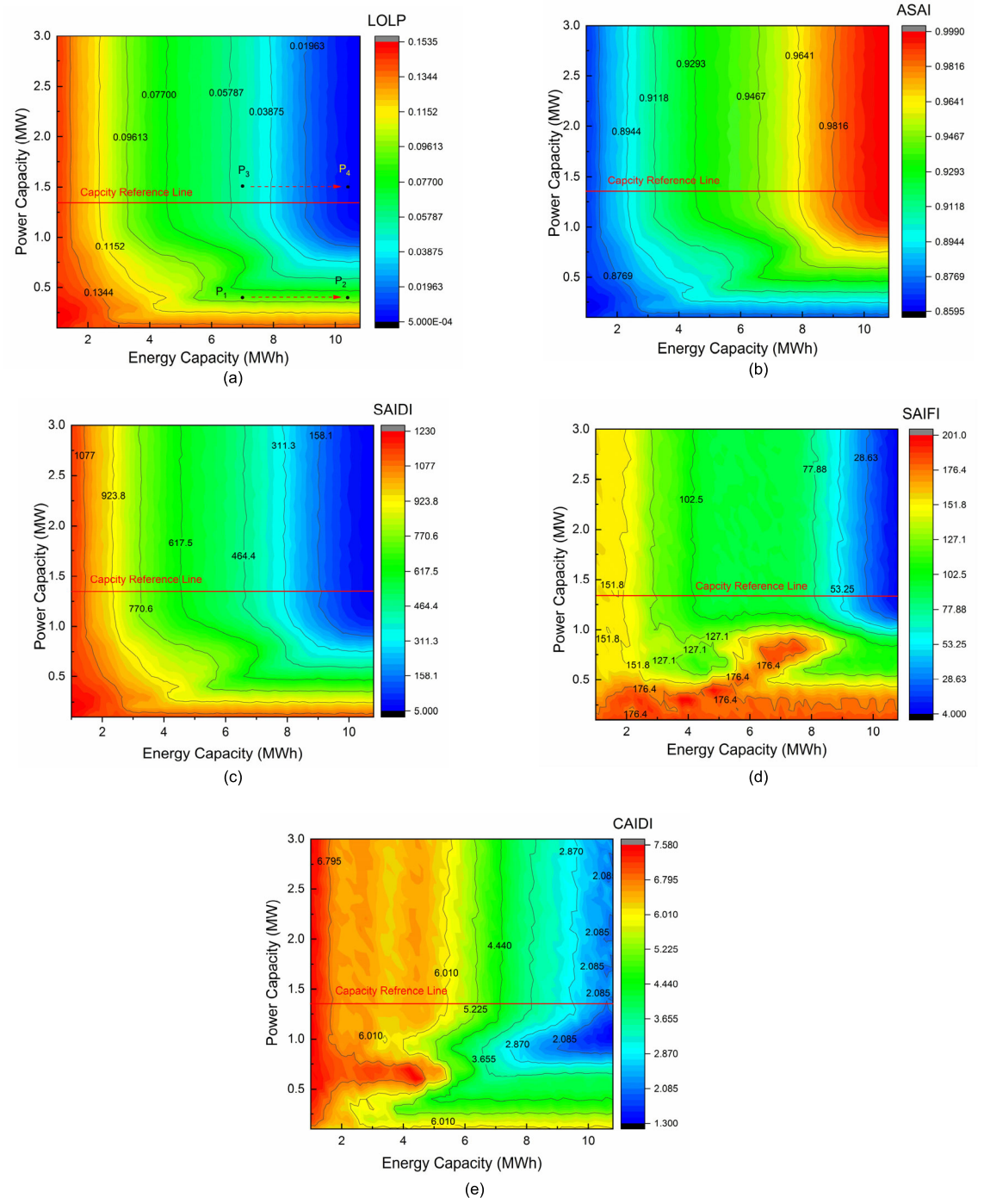

FIGURE 7. Reliability performance over varying energy capacity and power capacity of ESS: (a) along with increase of energy capacity, LOLP improves marginally when power capacity is lower than capacity reference line (e.g., from P_1 to P_2), but evidently when power capacity is higher than capacity reference line (e.g., from P_3 to P_4). Other indices, such as (b) ASAI, (c) SAIDI, (d) SAIFI and (e) CAIDI show characteristics similar to those of LOLP.

contour lines turn to horizontal direction gradually. Based on the investigation to the diagrams, the preferable sizes of ESS power and energy capacity can be determined from the viewpoint of reliability efficiency as below.

Assumed that the ESS power capacity is equal to EHRP, i.e., the value denoted by capacity reference line, reliability will be improved evidently and continuously along with the increase of ESS energy capacity, which can be determined by the requirement of reliability. Take SAIFI in Fig. 7(d) as an example, the ESS energy capacity should be no less than 9 MWh if SAIFI<53.25 *interruptions/customer. year* is required, with a ESS power capacity equal to EHRP as

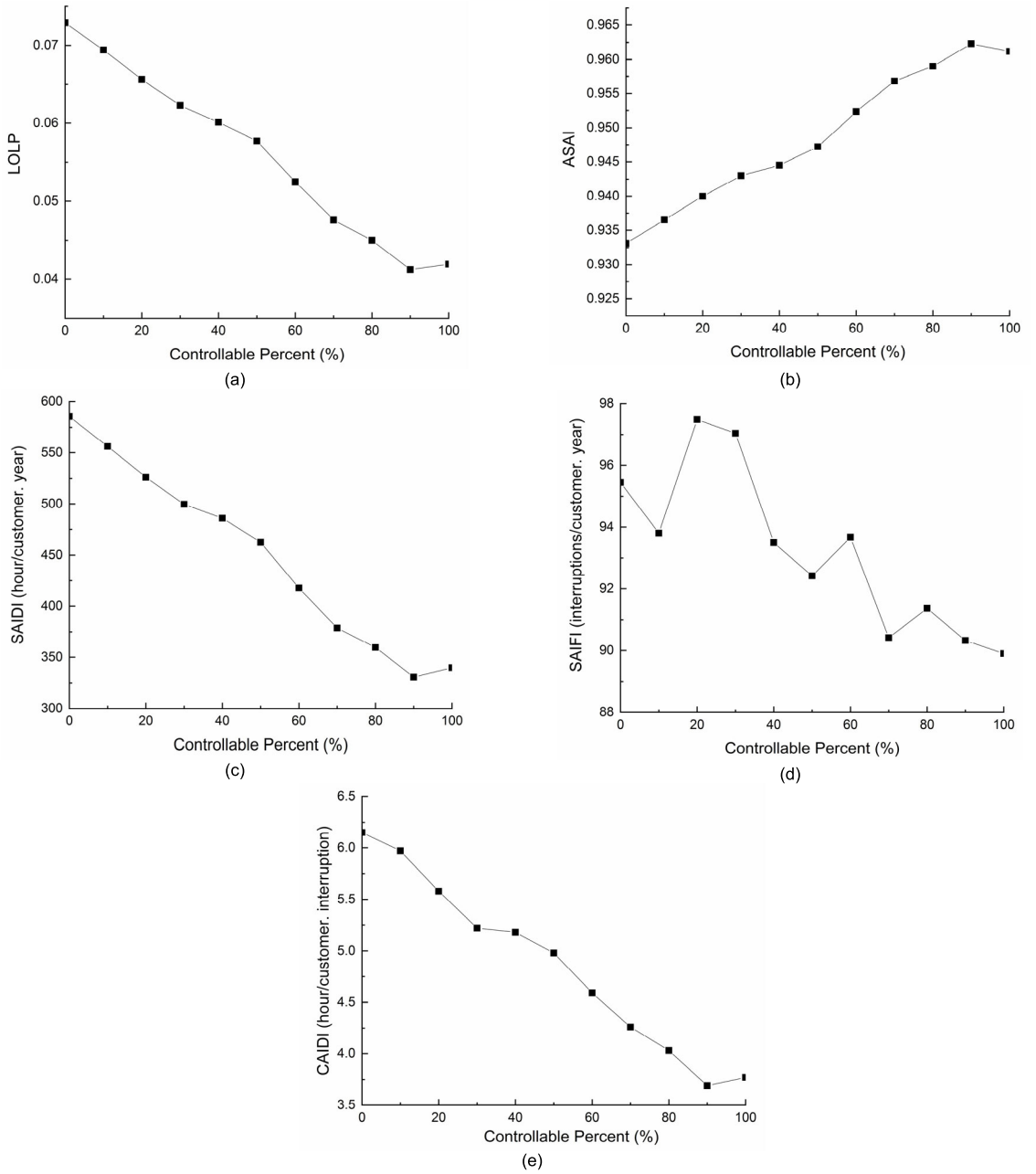

FIGURE 8. Reliability performance over different controllable percent of load: Curves of (a) LOLP, (b) ASAI, (c) SAIDI and (e) CAIDI present approximate linearity, different from curve of (d) SAIFI with fluctuations.

an prerequisite. Oversized power capacity of ESS which is much larger than EHRP is not preferable either due to the lower reliability efficiency. On the contrary, Undersized power capacity of ESS which is much lower than EHRP, will strongly constrain the reliability performance and its sensitivity to ESS energy capacity. It is suggested that ESS size can be determined by two steps:

(a) Work out EHRP as a reference of power capacity, and

(b) Determine the energy capacity by investigating the upper part of contour lines as shown in Fig. 7.

E. RELIABILITY PERFORMANCE OVER CONTROLLABLE LOADS

Controllable loads, such as air conditioner, electrical vehicles, etc., are playing an emerging but important role in the mitigation of load fluctuations. In order to perform the study on reliability performance over controllable loads, sizes of PV and ESS, are properly assumed in advance. PV capacity is assumed as 2.6 MW, identical to the value used in Subsection D, and the way in which PV capacity is determined has been explained above. According to the study in Subsection D, the assumed power capacity of ESS is equal

to EHRP, i.e., 1.352 MW to provide fair reliability efficiency of power capacity, and the ESS energy capacity is assumed thereafter as 5 MWh to present a reasonable benchmark of MG reliability. Here, LP_C is assumed as a partially controlled load point with a varying controllable percentage of load. The reliability indices over different controllable percentages of load are listed in Tab. 5, from which it can be seen that ASAI is improved evidently from 0.9331 to 0.9612, when the index of probability, for example is mentioned. At the same time, the index of frequency, SAIFI is improved from 95.45 to 89.90 *interruptions/customer. year*, and the index of duration, CAIDI is reduced from 6.15 to 3.77 *hours/customer. interruption*.

In addition, curves of reliability indices over controllable percentages of load are depicted in Fig. 8. Compared to varying characteristics of the reliability indices over sizes of PV and ESS, Fig. 8 shows approximate linear characteristics except the fluctuations of SAIFI curve, implying the notable reliability efficiency of load control. To draw a conclusion, load control should be no doubt considered delicately, especially when the reliability requirements cannot be met effectively by increasing the power supply or ESS sizes.

IV. CONCLUSION

In this paper, a framework of reliability assessment and varying characteristic analysis aiming at PV-ESS based standalone MG has been developed, by taking the sequential stochastic states of main components of MG, minimization of load shedding model, as well as CL model into consideration. we have conducted series of case studies and comprehensively investigated not only the indices of probability but also those of frequency & duration. The case studies have suggested that, first of all, increase of PV capacity will improve the indices of probability, but probably result in SE-SAIFI at the same time, especially when the ESS is undersized. However, SE-SAIFI can be avoided by properly deciding PV capacity to surpass the turning point, which is affected by the ESS sizes. Furthermore, EHRP have been worked out as a reference to reasonably determine the ESS power capacity, following with the decision of ESS energy capacity according to the requirement of reliability of MG. The solution of ESS size prompted by the novel method has provided reasonable balance between power and energy capacity. Lastly, most of the reliability indices under study have shown evident improvements due to the increase of controllable load, which have strongly validated the reliability efficiency of load control.

REFERENCES

[1] S. Parhizi, H. Lotfi, A. Khodaei, and S. Bahramirad, "State of the art in research on microgrids: A review," *IEEE Access*, vol. 3, pp. 890–925, Jul. 2015.
[2] J. Yu, C. Marnay, M. Jin, C. Yao, X. Liu, and W. Feng, "Review of microgrid development in the United States and China and lessons learned for China," *Energy Procedia*, vol. 145, pp. 217–222, Jul. 2018.
[3] A. Hirsch, Y. Parag, and J. Guerrero, "Microgrids: A review of technologies, key drivers, and outstanding issues," *Renew. Sustain. Energy Rev.*, vol. 90, pp. 402–411, Jul. 2018.
[4] H. Xie, S. Zheng, and M. Ni, "Microgrid development in China: A method for renewable energy and energy storage capacity configuration in a megawatt-level isolated microgrid," *IEEE Electrific. Mag.*, vol. 5, no. 2, pp. 28–35, Jun. 2017.
[5] P. Tiwari, M. Manas, P. Jan, Z. Nemec, D. Radovan, P. Mahanta, and G. Trivedi, "A review on microgrid based on hybrid renewable energy sources in South-Asian perspective," *Technol. Econ. Smart Grids Sustain. Energy*, vol. 2, no. 1, p. 10, Dec. 2017.
[6] R. Bayindir, E. Hossain, E. Bekiroglu, and E. Kabalci, " Microgrid facility at European union," in *Proc. 3rd Int. Conf. Renew. Energy Res. Appl.*, Milwaukee, WI, USA, Oct. 2014, pp. 865–872.
[7] X. Zhou and Q. Ai, "An integrated two-level distributed dispatch for interconnected microgrids considering unit commitment and transmission loss," *J. Renew. Sustain. Energy*, vol. 11, no. 2, 2019, Art. no. 025504. doi: 10.1063/1.5077032.
[8] A. Sadighmanesh, M. Sabahi, and M. Zavvari, "Probabilistic dispatch in hybrid-microgrid system with considering energy arbitrage," *J. Renew. Sustain. Energy*, vol. 11, no. 2, 2019, Art. no. 025904. doi: 10.1063/1.5081890.
[9] H. Jahangir, A. Ahmadian, M. Aliakbar-golkar, M. Fowler, and A. Elkamel, "Optimal design of standalone micro-grid considering reliability and investment costs," in *Proc. CIRED Workshop*, Helsinki, Finland, 2016, pp. 1–4.
[10] Y. Zhang, J. Wang, A. Berizzi, and X. Cao, "Life cycle planning of battery energy storage system in off-grid wind–solar–diesel microgrid," *IET Gener., Transmiss. Distrib.*, vol. 12, no. 20, pp. 4451–4461, Nov. 2018.
[11] S. Conti and S. A. Rizzo, "Monte Carlo simulation by using a systematic approach to assess distribution system reliability considering intentional islanding," *IEEE Trans. Power Del.*, vol. 30, no. 1, pp. 64–73, Feb. 2015.
[12] J. Mitra, M. R. Vallem, and C. Singh, "Optimal deployment of distributed generation using a reliability criterion," *IEEE Trans. Ind. Appl.*, vol. 52, no. 3, pp. 1989–1997, May/Jun. 2016.
[13] A. Khodaei, "Microgrid optimal scheduling with multi-period islanding constraints," *IEEE Trans. Power Syst.*, vol. 29, no. 3, pp. 1383–1392, May 2014.
[14] H. Farzin, M. Fotuhi-Firuzabad, and M. Moeini-Aghtaie, "A stochastic multi-objective framework for optimal scheduling of energy storage systems in microgrids," *IEEE Trans. Smart Grid*, vol. 8, no. 1, pp. 117–127, Jan. 2017.
[15] J. Mitra and M. R. Vallem, "Determination of storage required to meet reliability guarantees on island-capable microgrids with intermittent sources," *IEEE Trans. Power Syst.*, vol. 27, no. 4, pp. 2360–2367, Nov. 2012.
[16] L. H. Koh, P. Wang, F. H. Choo, K.-J. Tseng, Z. Gao, and H. B. Püttgen, "Operational adequacy studies of a PV-based and energy storage standalone microgrid," *IEEE Trans. Power Syst.*, vol. 30, no. 2, pp. 892–900, Mar. 2015.
[17] H. Farzin, M. Fotuhi-Firuzabad, and M. Moeini-Aghtaie, "Role of outage management strategy in reliability performance of multi-microgrid distribution systems," *IEEE Trans. Power Syst.*, vol. 33, no. 3, pp. 2359–2369, May 2018.
[18] T. Adefarati and R. C. Bansal, "Reliability and economic assessment of a microgrid power system with the integration of renewable energy resources," *Appl. Energy*, vol. 206, pp. 911–933, Nov. 2017.
[19] T. Adefarati and R. C. Bansal, "Reliability, economic and environmental analysis of a microgrid system in the presence of renewable energy resources," *Appl. Energy*, vol. 236, pp. 1089–1114, Feb. 2019.
[20] S. A. Arefifar and Y. A.-R. I. Mohamed, "DG mix, reactive sources and energy storage units for optimizing microgrid reliability and supply security," *IEEE Trans. Smart Grid*, vol. 5, no. 4, pp. 1835–1844, Jul. 2014.
[21] F. Azeem, G. B. Narejo, and U. A. Shah, "Integration of renewable distributed generation with storage and demand side load management in rural islanded microgrid," *Energy Efficiency*, pp. 1–19, Nov. 2018. doi: 10.1007/s12053-018-9747-0.
[22] R. R. Nejad and S. M. M. Tafreshi, "Operation planning of a smart microgrid including controllable loads and intermittent energy resources by considering uncertainties," *Arabian J. Sci. Eng.*, vol. 39, no. 8, pp. 6297–6315, 2014.
[23] M. Vahedipour-Dahraie, A. Anvari-Moghaddam, and J. M. Guerrero, "Evaluation of reliability in risk-constrained scheduling of autonomous microgrids with demand response and renewable resources," *IET Renew. Power Gener.*, vol. 12, no. 6, pp. 657–667, Apr. 2018.

[24] K. Hou, H. Jia, X. Xu, Z. Liu, and Y. Jiang, "A continuous time Markov chain based sequential analytical approach for composite power system reliability assessment," *IEEE Trans. Power Syst.*, vol. 31, no. 1, pp. 738–748, Jan. 2016.
[25] N. Shahidirad, M. Niroomand, and R.-A. Hooshmand, "Investigation of PV power plant structures based on Monte Carlo reliability and economic analysis," *IEEE J. Photovolt.*, vol. 8, no. 3, pp. 825–833, May 2018.
[26] J. R. Araújo, E. N. M. Silva, A. B. Rodrigues, and M. G. da Silva, "Assessment of the impact of microgrid control strategies in the power distribution reliability indices," *J. Control, Automat. Elect. Syst.*, vol. 28, no. 2, pp. 271–283, Apr. 2017.
[27] P. Wang and R. Billinton, "Time sequential distribution system reliability worth analysis considering time varying load and cost models," *IEEE Trans. Power Del.*, vol. 14, no. 3, pp. 1046–1051, Jul. 1999.
[28] L. Guo, Z. Yu, C. Wang, F. Li, J. Schiettekatte, J.-C. Deslauriers, and L. Bai, "Optimal design of battery energy storage system for a wind–diesel off-grid power system in a remote Canadian community," *IET Gener., Transmiss. Distrib.*, vol. 10, no. 3, pp. 608–616, Feb. 2016.
[29] H. Moradi, M. Esfahanian, A. Abtahi, and A. Zilouchian, "Modeling a hybrid microgrid using probabilistic reconfiguration under system uncertainties," *Energies*, vol. 10, no. 9, p. 1430, Sep. 2017.
[30] Y. Ying, Y. Wu, Y. Su, R. Fu, X. Liang, and H. Xu, "Dispatching approach for active distribution network considering PV generation reliability and load predicting interval," *J. Eng.*, vol. 2017, no. 13, pp. 2433–2437, Oct. 2017.
[31] N. Nikmehr and S. N. Ravadanegh, "Reliability evaluation of multi-microgrids considering optimal operation of small scale energy zones under load-generation uncertainties," *Int. J. Elect. Power Energy Syst.*, vol. 78, pp. 80–87, Jun. 2016.
[32] C. Battistelli, Y. P. Agalgaonkar, and B. C. Pal, "Probabilistic dispatch of remote hybrid microgrids including battery storage and load management," *IEEE Trans. Smart Grid*, vol. 8, no. 3, pp. 1305–1317, May 2017.
[33] D. J. Olsen, Y. Dvorkin, R. Fernández-Blanco, and M. A. Ortega-Vazquez, "Optimal carbon taxes for emissions targets in the electricity sector," *IEEE Trans. Power Syst.*, vol. 33, no. 6, pp. 5892–5901, Nov. 2018.
[34] C. Wang, T. Zhang, F. Luo, F. Li, and Y. Liu, "Impacts of cyber system on microgrid operational reliability," *IEEE Trans. Smart Grid*, vol. 10, no. 1, pp. 105–115, Jan. 2019.
[35] S. A. Arefifar, Y. A.-R. I. Mohamed, and T. H. M. EL-Fouly, "Optimum microgrid design for enhancing reliability and supply-security," *IEEE Trans. Smart Grid*, vol. 4, no. 3, pp. 1567–1575, Sep. 2013.
[36] R. Billinton and S. Jonnavithula, "A test system for teaching overall power system reliability assessment," *IEEE Trans. Power Syst.*, vol. 11, no. 4, pp. 1670–1676, Nov. 1996.
[37] B. Zhou, T. Huang, and Y. Zhang, "Reliability analysis on microgrid considering incentive demand response," (in Chinese), *Automat. Electr. Power Syst.*, vol. 41, no. 13, pp. 70–78, Jul. 2017.

XIAOTONG SONG received the B.Eng. and Ph.D. degrees in electrical engineering from Shandong University, Jinan, China, in 2003 and 2008, respectively.

He was a Senior Engineer with the China Electric Power Research Institute (CEPRI). He is currently an Associate Professor with the School of Electrical and Control Engineering, North China University of Technology (NCUT), Beijing, China. His research interests include power system reliability assessment, microgrid, and energy storage systems.

Dr. Song was a recipient of the Grand Prize of State Grid Awards for Science and Technology Progress, in 2013.

YUXIN ZHAO was born in Heilongjiang, China, in 1995. She received the B.Eng. degree in electrical engineering and its automation from Heilongjiang Bayi Agricultural University, Daqing, China, in 2018. She is currently pursuing the M.S. degree in electrical engineering with the North China University of Technology (NCUT). Her research interests include optimal dispatch of microgrid and distributed generation.

JINGHUA ZHOU received the Ph.D. degree in electrical engineering from the School of Electrical Engineering, Xi'an Jiaotong University, Xi'an, China, in 2005. He is currently a Professor with the School of Electrical and Control Engineering, North China University of Technology (NCUT), Beijing, China. His research interests include power electronics, renewable energy, and microgrid.

ZHIPENG WENG received the B.Eng. degree in electronic information science and technology from the College of Technology, Hubei Engineering University, Hubei, China, in 2015. He is currently pursuing the M.S. degree in electrical engineering with the North China University of Technology (NCUT). His research interest includes the reliability evaluation of microgrid.